Accurate Rover Mobility Analysis Using HILS-DRFT with Real-Time Parameter Tuning Approach

Takahiro Fuke, Sora Ishikawa and Genya Ishigami

October 6, 2024

2919 | Accurate Rover Mobility Analysis Using HILS-DRFT with Real-Time Parameter Tuning Approach

Takahiro Fuke [a,*], Sora Ishikawa [a], Genya Ishigami [a]

[a] *Department of Mechanical Engineering, Keio university, Yokohama, Japan*

* *Corresponding author: taka162uke@keio.jp*

A B S T R A C T

Offroad mobility in extraterrestrial exploration can be significantly degraded by vehicle slippage on soft terrain covered with fine powdery sand known as regolith. Comprehensive design analysis and verification of the rover's mobility have been widely investigated using numerical and experimental approaches. Numerical simulations for the mobility analysis require accurate modeling of the contact forces between the wheel and sand. While several wheel-sand interaction models have been proposed based on the Bekker-Wong-Reece theory, the Dynamic Resistive Force Theory (DRFT) proposed in the early 2020s is a notable approach for its low computational cost and adaptability to quasi-dynamic motion. The scaling factor used in DRFT is the only parameter for representing sand-dependent parameters, and its value needs to be empirically tuned to achieve accurate and reliable mobility analysis. Therefore, the authors have integrated a single-wheel test bed into a closed-loop Hardware-In-the-Loop Simulation (HILS) associated with DRFT. This HILS-DRFT experimentally observes the characteristics of the wheel sinking phenomenon in the wheel test bed, and then, the value of the scaling factor is tuned in real-time by the difference between the observed wheel sinkage and the DRFT simulation. This real-time parameter tuning method accurately reproduces wheel mobility, particularly in its transient states, which were previously unachievable with DRFT alone. The proposed HILS-DRFT with the real-time tuning method will contribute to the efficient and reliable development of rovers.

Keywords
Terramechanics
Resistive Force Theory
Hardware-In-the-Loop Simulation

1. Introduction

Extraterrestrial exploration missions hold immense scientific significance in unraveling the processes involved in the evolution of the solar system. Furthermore, the valuable data obtained through the exploration plays a crucial role in establishing bases for expanding domain of human activities. The use of rovers capable of freely traversing the planetary surface enables the collection of more detailed sample data. However, the terrain surface is composed of a soft terrain covered with fine powdery sand known as regolith that often degrade the rover mobility performance due to slippage. Therefore, it is necessary to thoroughly test the rover's traversal performance before sending to other planets.

Comprehensive design analysis and verification of the rover's mobility have been widely investigated using both experimental and numerical approaches. Notably, numerical methods using semiempirical terramechanics model have long been researched for their potential to reduce the cost of empirical validation. The Bekker-Wong-Reece theory (Bekker, 1956,1960, 1969; Wong, 2008; Wong and Reece, 1967) forms the foundation upon which various wheel-sand interaction models have been developed. However, these models face challenges such as the necessity to consider for numerous sand parameters, their inability to accommodate complex wheel shapes and high-speed motion. In response to these challenges, the Dynamic Resistive Force Theory (DRFT) (Agarwal et al., 2021) was proposed by applying the Resistive Force Theory (RFT) (Li et al., 2013) which divides the wheel's surface into minute plates. The RFT uses the only one sand parameter called scaling factor. The RFT is advantageous as it can be applied to wheels with complex shapes and in wide range of speed. However, this method cannot accurately simulate transient states because the dynamic change of wheel-sand interaction mechanics varies the sand stiffness or the value of the scaling factor.

Therefore, we have integrated a single-wheel test bed into a closed-loop Hardware-In-the-Loop Simulation (HILS) associated with DRFT (Ishikawa et al., 2022). This HILS-DRFT experimentally observes the characteristics of the wheel sinking phenomenon in the wheel test bed, and then, the value of the scaling factor is tuned in real-time based on the difference between the observed wheel sinkage and the DRFT simulation. In this paper, we show the concept of this HILS-DRFT proposed by Ishikawa and demonstrate the validity through comparative experiments on sandy terrain.

2. Overview of HILS-DRFT

2.1. Overview of HILS

Figure 1 shows the general framework of the HILS. Compared to a full software simulation for a target system, the HILS replaces part of the numerical model with an actual experiment using a hardware testbed. The hardware testbed of the HILS measures a real phenomenon of the part of the system in a hardware environment. Subsequently, in a software environment, the numerical model calculates the system's response based on the measured values. The HILS continuously loops these experimental measurements and numerical calculations as the temporal behavior of the system progresses. The HILS is particularly useful in cases where the actual phenomenon of a target system is difficult to measure or where an accurate numerical model is barely available.

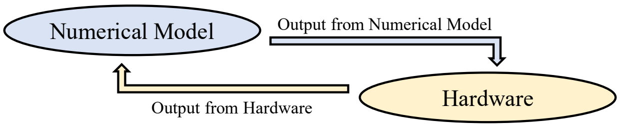

Fig. 1. Simplified flowchart of HILS

2.2. Overview of DRFT

2.2.1. Basics of RFT

The RFT is a modeling technique that divides the surface of an object into small plates, as illustrated in *Fig. 2*.

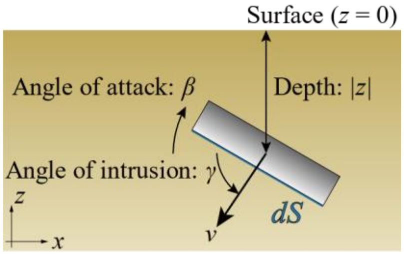

Fig. 2. Definitions of plate element's variables

Here, $\mathrm{d}S$ is the contact surface of each plate, $|z|$ is the depth from the sand surface, β is the attack angle, and γ is the intrusion angle. Both β and γ range from $-\pi/2$ to $\pi/2$, with their starting points and positive directions indicated by the arrows in *Fig. 2*. Under this definition, the contact force per unit area $\boldsymbol{\sigma}(\beta,\gamma,|z|)$ that each plate receives from the sand is expressed as follows:

$$\boldsymbol{\sigma}(\beta,\gamma,|z|) = \zeta\boldsymbol{\alpha}^{\text{generic}}(\beta,\gamma)|z| \tag{1}$$

Here, ζ is a dimensionless sand parameter called the scaling factor, determined by properties such as grain shape and packing density of the sand, and $\boldsymbol{\alpha}^{\text{generic}}(\beta,\gamma)$ is a function experimentally identified (Li., et al 2013). With this $\boldsymbol{\sigma}(\beta,\gamma,|z|)$ and $\mathrm{d}S$, the contact force $\mathrm{d}\boldsymbol{F}$ acting on each plate can be calculated as follows:

$$\mathrm{d}\boldsymbol{F} = \boldsymbol{\sigma}(\beta,\gamma,|z|)\mathrm{d}S \tag{2}$$

Finally, by summing up the contact force $\mathrm{d}\boldsymbol{F}$ acting on each plate over the contact surface S, the total contact force $\boldsymbol{F}$ acting on the entire object can be calculated as follows:

$$\boldsymbol{F} = \int_S \mathrm{d}\boldsymbol{F} = \int_S \boldsymbol{\sigma}(\beta,\gamma,|z|)\mathrm{d}S = \int_S \zeta\boldsymbol{\alpha}^{\text{generic}}(\beta,\gamma)|z|\mathrm{d}S \tag{3}$$

2.2.2. DRFT for modeling wheel-sand interaction

It has been pointed out that contact force calculated from the original RFT deviates from actual results when applied to modeling wheel - sand interaction. To address this issue, (Agarwal et al., 2021) proposed DRFT that considers the following factors:

1. The momentum flux of the granular media.
2. The height decrease behind the wheel.

The momentum flux of the granular media is considered by adding $-\lambda\rho v_n^2$ to the RHS of *Eq. 1* where λ, ρ and v_n respectively represent the fitting coefficient, the bulk density of the granular media and the normal component of the plate's velocity $\boldsymbol{v}$. Introducing the outward unit normal $\boldsymbol{n}$ to each plate surface, v_n is represented by $\boldsymbol{n}\cdot\boldsymbol{v}$. The height decrease occurs behind the wheel is considered by substituting $|z|$ in the RHS of *Eq. 1* with the effective depth $|\tilde{z}|$, defined as follows:

$$|\tilde{z}| = \begin{cases} |z| - \delta h \text{ (for plates in } \theta_r) \\ |z| \text{ (for plates in } \theta_f) \end{cases} \tag{4}$$

$$\delta h = r\left(\frac{r\omega^2}{g}\right) \tag{5}$$

Here, δh is the height decrease behind the wheel, r is the wheel radius, ω is the angular velocity of the wheel, and g is the gravitational acceleration. Additionally, as illustrated in *Fig. 3*, θ_r and θ_f represent the angles that bisect the contact surface S..

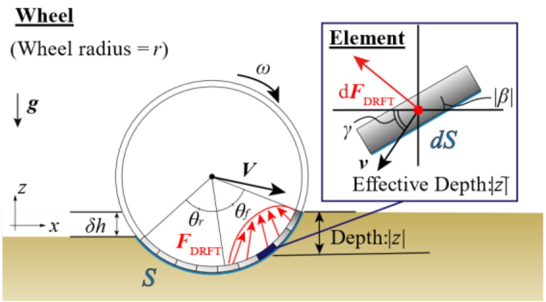

Fig. 3. Modeling of the wheel – sand interaction according to DRFT

Considering these two, the net force $\boldsymbol{F}_{\text{DRFT}}$ is given as follows:

$$\boldsymbol{F}_{\text{DRFT}} = \int_S \left(\zeta\boldsymbol{\alpha}^{\text{generic}}(\beta,\gamma)|z| - \lambda\rho v_n^2\boldsymbol{n}\right)\mathrm{d}S \tag{6}$$

2.3. Hardware test bed of HILS-DRFT

The single-wheel test bed illustrated in *Fig. 4* served as the hardware test bed. This apparatus, measuring 3500 mm in total length (2500 mm travelable length) and 600 mm in width, features horizontal, vertical, and rotational axes for the wheel. The horizontal axis includes a linear motion mechanism consisting of a motor, ball screw, and linear guide. The vertical axis comprises a passive-sliding mechanism with a linear guide, while the wheel's rotational axis incorporates a motor and a gearhead. The wheel, along with the moving frame, can travel both horizontally and vertically. The moving frame connects to the ball screw via a ball screw nut, allowing for the recreation of various wheel slipping conditions. Additionally, by disengaging the ball screw nut, it is possible to observe the travel controlled solely by the wheel's rotation. Magnetic scales attached to the linear guides in both directions measure displacement from the initial position horizontally and vertically. The apparatus uses Toyoura standard sand (average grain size 0.11 mm), ensuring high reproducibility due to its uniform grain size and shape.

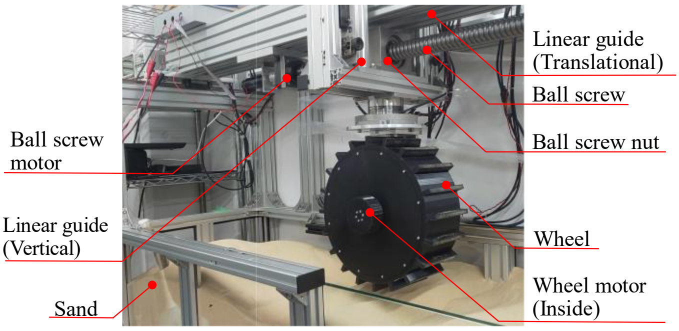

Fig. 4 Overview of single-wheel test bed

2.4. Framework of HILS-DRFT

Figure 5 illustrates the HILS-DRFT framework. This framework is almost identical to our previous works (Ishikawa et al., 2022), except the current framework omits the force measurements. In general, the scaling factor representing terrain stiffness is treated as a constant during numerical simulations; however, the HILS-DRFT framework assumes that it is dynamically varied. Here, $\boldsymbol{x}_{\mathrm{tw}}$, $\boldsymbol{v}_{\mathrm{tw}}$, and $\boldsymbol{F}_{\mathrm{tw}}$ are vectors with components in the horizontal x and vertical z directions, representing the position vector of the wheel's center of mass, the velocity vector, and the contact force exerted by the sand on the wheel, respectively. The initial conditions required at the start of the simulation include the wheel's static sinkage H_{static}, the initial value of the scaling factor $\zeta(0)$, the wheel's initial position $\boldsymbol{x}_{\mathrm{tw}}(0)$, and the wheel's initial velocity $\boldsymbol{v}_{\mathrm{tw}}(0)$. Only the angular velocity ω is controlled externally. Notably, the wheel operates simultaneously in both the computer environment and the wheel test bed. In this setup, only the wheel's angular velocity ω and the horizontal component of the translational velocity $v_{\mathrm{tw},x}$ are sequentially provided to the single-wheel test bed, with no direct involvement in the vertical motion. This enables real-time tuning of the scaling factor $\zeta(t)$ based on the difference between the dynamic sinkage values H_{sim} and $\boldsymbol{H}_{\mathrm{real}}$ obtained from each environment.

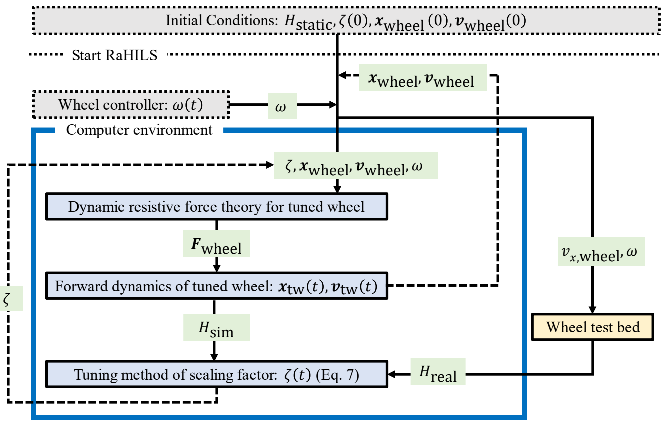

Fig. 5. Framework of HILS-DRFT

Specifically, tuning method of scaling factor in *Fig. 5* follows the equation outlined below:

$$\zeta(t+1)=\begin{cases}\zeta(t)+\Delta\zeta & (H_{\mathrm{real}}-H_{\mathrm{sim}}<-\epsilon)\\ \zeta(t)-\Delta\zeta & (H_{\mathrm{real}}-H_{\mathrm{sim}}>\epsilon)\\ \zeta(t) & (|(H_{\mathrm{real}}-H_{\mathrm{sim}})|\le\epsilon)\end{cases} \tag{7}$$

Here, $\Delta\zeta$ represents the incremental change in the scaling factor per tuning, and ϵ represents the allowable error. By appropriately setting these values, stable and precise behavior analysis becomes possible. In this study, $\Delta\zeta$ was set to 0.001 and ϵ was set to 0.1 mm.

3. Experiment

3.1. Experimental setup

As previously mentioned, the single-wheel test bed can be operated in a state where the horizontal moving frame is disconnected from the ball screw, allowing the wheel to move solely through its own rotation. This type of single-wheel driving experiment is referred as *Experiment driving* or ground truth data. In contrast, a single-wheel driving experiment using the HILS-DRFT framework will be referred as *HILS-DRFT driving*. Additionally, as shown in *Fig. 5*, two different trajectories of wheels can be observed in HILS-DRFT: one from the numerical model in a computer environment and the other from the real single-wheel testbed. We refer to the former as *HILS-DRFT (sim)* and the latter as *HILS-DRFT (real)*.

To ensure accurate comparisons, unified conditions are presented in *Tables 1 and 2*. Here, we differentiate between the horizontal and vertical masses, denoted as m_x and m_z , respectively. This distinction is necessary because the horizontal moving frame in the single-wheel test bed does not influence vertical motion. Properly setting these parameters is essential to ensure the accuracy of the forward dynamics solved in the computer environment. The initial conditions used for the HILS-DRFT framework are shown in *Table 3*, and they were configured based on the observed initial conditions from the *Experiment driving*.

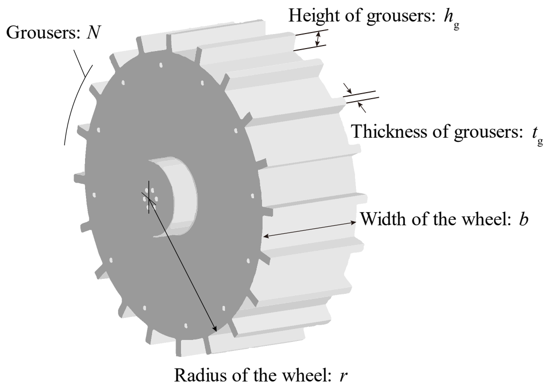

Fig. 6. Illustration of the wheel with grousers

Table 1
Typical unified parameters between HILS-DRFT and experiment

Parameters	Values
Radius of wheel r [m]	0.150
Width of the wheel b [m]	0.120
Number of grousers N [-]	12
Height of grousers h_g [m]	0.018
Thickness of the grousers t_g [m]	0.009
Horizontal mass m_x [kg]	13.902
Vertical mass m_z [kg]	18.837
Angular velocity profile of the wheel control	(Shown in *Table 2*)

Table 2
Angular velocity profile of the wheel control

Time [s]	Wheel state	ω [deg/s]
0 → 2	*Stand by*	0
2 → 7	*Constant acceleration rotation*	0→30
7 → 17	*Constant rotational speed*	30
17 → 22	*Constant deceleration rotation*	30→0
22 → 24	*Stand still*	0

Table 3
Initial conditions used for HILS-DRFT

Variables	Values
Static sinkage H_{static} [m]	0.0176
Initial scaling factor $\zeta(0)$ [-]	0.7823
Initial position $\boldsymbol{x}_{\mathrm{tw}}(0)$ [m]	$(0.0,-H_{\mathrm{static}})$
Initial velocity $\boldsymbol{v}_{tw}(0)$ [m/s]	(0.0,0.0)

3.2. Validation of tuning method in HILS-DRFT

The single-wheel experiment result verifies how the real-time tuning of the scaling factor appropriately works. One typical result of the HILS-DRFT is shown in *Fig. 7*. The vertical axis represents the wheel's displacement in the wheel vertical direction Δz, and the horizontal axis represents time t. Qualitatively, the sinkage of *HILS-DRFT (sim)* matches the sinkage of *HILS-DRFT (real)*. Additionally, the same experiment was executed ten times, and the root mean square error (RMSE) of Δz was less than 1 mm in all cases, which is remarkably small to the wheel radius. Also, the plot shows oscillations. To investigate the cause of these oscillations, we conducted an FFT analysis on the time variation of the settlement during *Constant rotational speed* running, and the result showed a peak at about 1.68 Hz. Considering that the wheel has 12 grousers and a rotational angular velocity of 30 degrees per second, this frequency characteristic is consistent with the influence of the wheel grousers, which is also observed in *Experiment driving*. These findings indicate that the oscillations are not due to the discreteness of the parameter tuning method proposed in this paper but rather the periodicity of the wheel grousers. Thus, the real-time tuning of the scaling factor functions appropriately.

Observing the changes in the scaling factor, we can see that it decreases from the beginning to the end of the wheel's rotation. As mentioned earlier, the scaling factor represents the terrain stiffness, so this indicates that the sand around the wheel becomes looser compared to its static state. This loosening is likely caused by the wheel's rotation, which excavates the sand. This result also implies that the value of the scaling factor is not constant and that should be tuned for static/dynamic states accordingly.

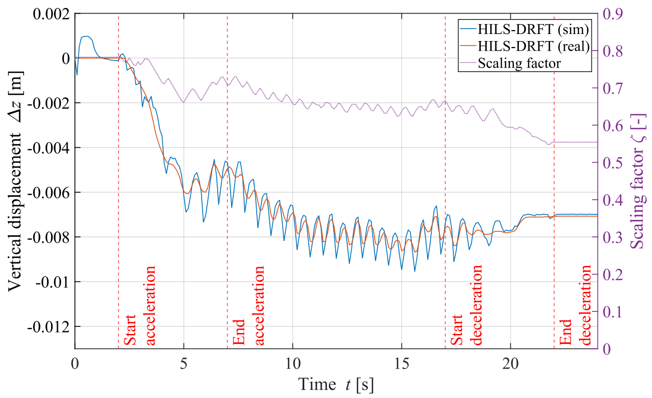

Fig. 7. Result of HILS-DRFT focused on real time tuning method

3.3. Compare the result of HILS-DRFT and DRFT

This subsection evaluates the accuracy of *HILS-DRFT driving* in replicating *Experiment driving*. Ten runs were conducted for both *Experiment* and *HILS-DRFT driving*. *Figure 8* illustrates the wheel trajectories for *Experiment driving*, *HILS-DRFT driving*, and original DRFT for comparison. For *HILS-DRFT driving*, two sets of results are available: *HILS-DRFT (sim)* and *HILS-DRFT (real)*. However, only the *HILS-DRFT (sim)* results are presented here. Each plot shows the mean values of the ten runs with solid lines, and the standard deviations are indicated with light shading. The vertical axis represents the wheel's vertical displacement, Δz, and the horizontal axis represents the wheel's horizontal displacement, Δx. The results indicate that HILS-DRFT can simulate transient states more accurately than DRFT. Additionally, when comparing the RMSE of the average trajectory between *Experiment driving* and both *HILS-DRFT driving* and original DRFT, the values are 5.0 mm and 8.4mm, respectively. Therefore, HILS-DRFT demonstrates superior accuracy over DRFT not only in transient states but also in other conditions.

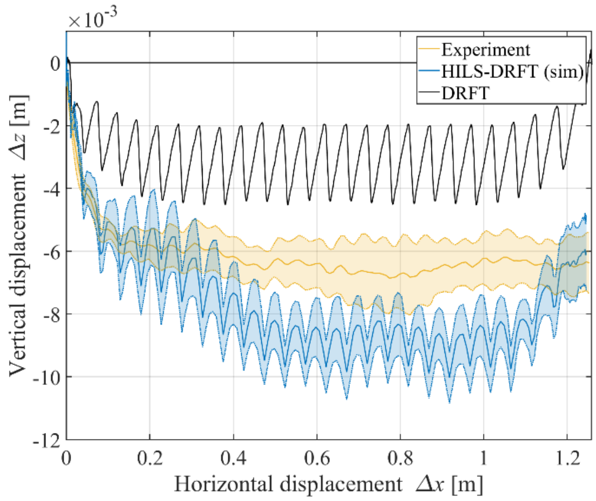

Fig. 8. Wheel trajectories of experiment, HILS-DRFT and original DRFT

However, a small error remains. By tuning the coefficients of the damping terms added to the forward dynamics for stabilizing HILS, more stable calculations and reduced errors can be achieved.

4. Conclusions and future work

This study evaluated the HILS-DRFT framework's effectiveness. The framework employs a real-time tuning method for sand parameters based on sinkage observed in a single-wheel test bed. During verification, results from the original DRFT and HILS-DRFT were compared with actual driving results. The comparison demonstrated that HILS-DRFT behavior closely matched actual wheel performance, surpassing the original DRFT. It was also notably accurate in simulating the transient state.

The tuning of the scaling factor does not merely involve fitting arbitrary parameters to align experiments with simulations. Instead, it sequentially identifies terrain stiffness caused by sand flow, compaction, and compression due to the wheel's movement. This method is applicable to analyzing vehicles with multiple wheels. Future research should extend the HILS-DRFT framework to analyze rovers' actual driving behavior, achieving more precise results.

5. Declaration of competing interest

The authors declare that they have no known competing financial interests or personal relationships that could have appeared to influence the work reported in this paper.

6. References

Agarwal, S., Karsai, A., Goldman, D.I., Kamrin, K., 2021. Surprising simplicity in the modeling of dynamic granular intrusion. Sci. Adv. 7, eabe0631.
Bekker, M.G., 1956. Theory of land locomotion. University of Michigan Press, Ann Arbor.
Bekker, M.G., 1960. Off-the-road locomotion University of Michigan Press, Ann Arbor.

Bekker, M.G., 1969. Introduction to terrain-vehicle systems. University of Michigan Press, Ann Arbor.

Ishikawa, S., Ishigami, G., 2022. Development of Hardware-in-the-loop Simulator for Rough Terrain Mobile Robot and Its Application to Real-time Tuning of Wheel Dynamics Model. Journal of the Robotics Society of Japan. 40, 542-545.

Li, C., Zhang, T., Goldman, D.I., 2013. A terradynamics of legged locomotion on granular media. Science 339, 1408–1412.

Wong, J.Y., Reece, A., 1967. Prediction of rigid wheel performance based on the analysis of soil-wheel stresses part I. performance of driven rigid wheels. J. Terramech. 4, 81-98.

Wong, J.Y., Reece, A., 1967. Prediction of rigid wheel performance based on the analysis of soil-wheel stresses part II. performance of driven rigid wheels. J. Terramech. 4, 7-25.

Wong, J.Y., 2008. Theory of ground vehicles. Hohn Wiley & Sons Inc., Hoboken, New Jersey.